Effect of recaesiation on quantum efficiency recovery for GaN photocathodes

LINGAI SU[a], YANG SHEN[a], LIANG CHEN[a,b,*], YUNSHENG QIAN[b], SUNAN XU[a], SHUQIN ZHANG[a]
[a]*Institute of Optoelectronics Technology, China Jiliang University, 310018, Hangzhou, China*
[b]*Institute of Electronic Engineering & Optoelectronics Technology, Nanjing University of Science and Technology, 210094, Nanjing, China*

Using the first-principles plane-wave pseudo-potential method based on density functional theory (DFT), the work function and band structure of five different (1×1) GaN (0001) surface models are calculated in this paper. To investigate the recovery status of the quantum efficiency (QE) of reflection-mode NEA GaN photocathode, the QE curves have been studied after the photocathode was fully activated, stored in system and supplement with Cs. The results show that there is a good recovery on the overall curve, the short wavelengths below 300nm recover better, and those long ones excess 300nm can also recover up to 88% after supplement with Cs. Our calculation results are well consistent with the experimental analysis, indicating the explanation is proper and instructive.

(Received June 3, 2015; accepted November 25, 2016)

Keywords: Quantum efficiency, Negative electron affinity (NEA), Reflection-mode, GaN photocathode, Recovery status

1. Introduction

As the well known third-generation semiconductor materials after Ge, Si, GaAs, and InP, GaN and III-Vmaterials are recently used to develop microelectronic devices and optoelectronic devices, such as vacuum electron sources, and ultraviolet detectors [1-3].GaN ultraviolet photocathode based on negative electron affinity (NEA) possess fascinating properties such as wide band gap, high sensitivity, high quantum efficiency distribution, high solar blind response, low dark current, and have promising application future in flat electronic printing and vacuum ultraviolet detection [4-9]. These fields need GaN photocathode higher sensitivity, better photoemission performance, and longer lifetime. In other words, the quantum efficiency (QE) stability must be guaranteed. QE is an important parameter that shows the photocathode characteristics, and allows us to understand the photoelectric emission mechanisms. Furthermore, it can be used to quantify the photocathode photoelectric emission performance. Though some experiments have been carried out on the NEA GaN photocathode QE [10-13], a theoretical study on the QE recovery mechanism after decay of reflection-mode NEA GaN photocathode is still required.

It is inevitable to research the factors of GaN photocathode QE recovery mechanism for the current study on NEA GaN photocathode. Prolonging NEA GaN lifetime as far as possible is necessary for its applications. In this paper, we carried out experiments on the reflection-mode NEA GaN photocathode, through observing its QE decay characteristics and researching cathode QE recovery status after supplement with Cs, the GaN photocathode QE recovery mechanism was found out. Qiao et al. [14] reported the decay tendency and the recovery status of the QE of reflection-mode NEA photocathode. In this paper, we made experiments and calculation on the reflection-mode NEA GaN photocathode, at the same time, the calculation based on the first principle verified the recovery status of QE.

2. Calculation method and models

All calculations in the paper were performed with the quantum mechanics program Cambrige Serial Total Energy Package (CASTEP) code [15]. The plane-wave ultra-soft pseudopotential method based on density functional theory (DFT) [16] within the generalized-gradient approximation (GGA) [17] was used. The Broyden–Fletcher–Goldfarb–Shanno (BFGS) algorithm was used to relax the structure of the crystal model [18]. All calculations were carried in reciprocal space with Ga: $3d^{10}4s^24p^1$, N: $2s^22p^3$, Cs: $5s^25p^66s^1$, O: $2s^22p^4$ and H: 1s as the valence electrons. The valence electronic wave function was expanded in a plane wave basis vector. After a series of tests, the final set of energies was computed with an energy cutoff of 400eV. The convergence precision was set to energy change less than 2×10^{-6}eV/atom, other parameters were set as follows: force less than 0.005eV, stress less than 0.05GPa, the convergence tolerance of a single atomic energy below

1×10^{-5}eV/atom, and change in displacement less than 1×10^{-5}nm in iterative process. The Brillouin zone integral is sampled with the Monkhorst-Pack mesh scheme and special k points of high symmetry. The number of k points for GaN (0001) surface is set as 9×9×1.

The wurtzite GaN has a hexagonal structure, which belongs to the P63-MC space group. The lattice constant can be described with a=b=0.3189nm, c=0.5185nm [19], α=β=90°, γ=120°. As depicted in Fig. 1 (a), the surface slab models are modeled with 12 layers of atoms (six Ga-N layers) to simulate (1×1) GaN (0001) surface. The top three layers of GaN (0001) slab model are relaxed freely and the bottom three layers are fixed. A vacuum thickness of 15Å is used to avoid interaction between repeated slabs.

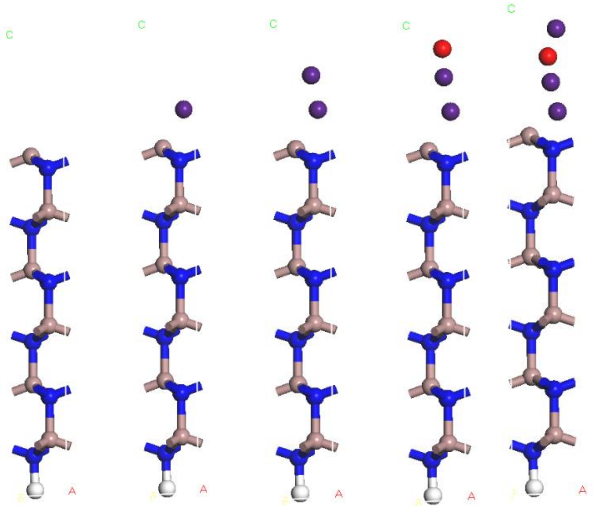

(a) (b) (c) (d) (e)

Fig. 1. (a) Clean (1×1) GaN (0001) surface model, (b) GaN (0001)-Cs surface model, (c) GaN (0001)-Cs-Cs surface model, (d) GaN (0001)-Cs-Cs-O surface model, (e) GaN (0001)-Cs-Cs-O-Cs surface model

3. Analyses and discussions

3.1. Changes of work function caused by Cs, O adsorption and recaesiation

For semiconductors, photoemission of NEA photocathode can be described as a three-step process of optical absorption in bulk, electrons transport from bulk to the surface, and escape across the surface into vacuum by Spicer in 1958 [19], the third step mainly depends on work function. Work function is defined by the following formula [20]:

$$\phi = E_{vac} - E_f \tag{1}$$

Where, E_{vac} is the energy level of vacuum and E_f represents the Fermi level of the surface. It suggests that the work function is the minimum energy needed by electrons at the bottom to escape across the surface into vacuum. The work functions of different surface models are shown in Table 1. The work function values are calculated and analyzed. In Table 1, the work function value of clean GaN (0001) surface is 4.38 eV, which is in good agreement with the value [21], in keeping with theory conclusion.

Table 1. The calculated values of work function for different surface models: "+" represents increment, "−" represents decrement

Surface model	a	b	c	d	e
ϕ	4.38	2.52	2.59	6.49	1.59
$\Delta\phi$		-1.86	+0.07	+3.90	-4.90

From Table 1, it can seen that when one Cs atom adsorbed at the N top on the surface of (1×1) GaN (0001) (picture (b) in Fig. 1), the calculated work function was 2.52eV, which was lower than the clean (1×1) GaN (0001) surface (picture (a) in Fig. 1). The main reason for the work function reducing caused by Cs adatom is that the electronegativity of Ga atom is larger than that of Cs atom, thus Cs atom losing electrons to Ga atom and form surface dipole moment which is depicted in Fig. 2 (a). And then they form the first dipole layer (GaN-Cs) with GaN, which will broaden the surface band structure, the vacuum energy decreasing to 2.52eV. As another Cs atom adsorbed on the top of Cs atom on the surface of (1×1) GaN (0001) (picture (c) in Fig. 1), the work function became 2.59eV after relaxation, which is a bit higher than model (picture (b) in Fig. 1). It can be explained as this: with the increase of Cs coverage, the interaction between Cs atoms increases and distance between Cs atoms decreases, then electrons in the GaN (0001) surface and Cs atoms redistribute to achieve equilibrium, in other words, some electrons return to Cs atoms from GaN (0001) surface. As a result, the dipole moments between Cs atoms and GaN (0001) surface decrease, resulting in work function increasing. When one O atom was absorbed on the top of Cs atom, as shown in model d (picture (d) in Fig. 1), the work function changed to 6.49eV, larger than model c (picture(c) in Fig. 1). This can be attributable to that the electronegativity of Cs atom is smaller than that of O atom, O atom got electrons and formed a downward dipole moment the second adsorption with Cs atom, which weakened the original dipole moment, thus causing work function increasing. As shown in model e (picture (e) in Fig. 1), the work function was 1.59eV when another Cs atom absorbed, which decreased greatly compared with model d (picture (d) in Fig. 1), this is mainly because the second dipole layer (O-Cs) was formed, which resulted in the work function declining further.

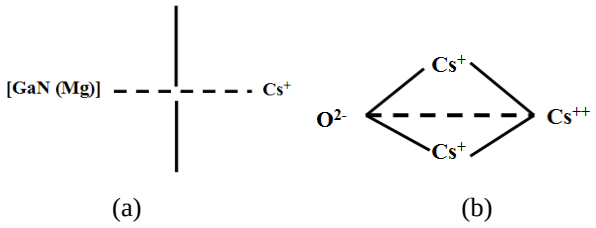

Fig. 2. The formation of (a) [GaN (Mg): Cs] dipole and (b) Cs-O dipole

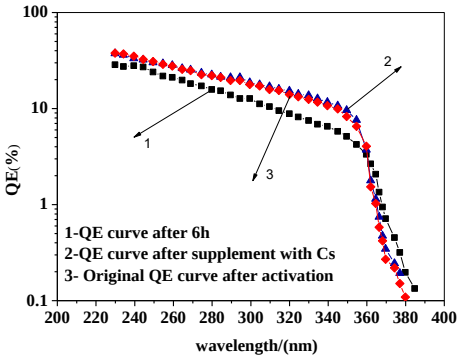

Fig. 3. Variation curves of quantum efficiency of NEA GaN photocathode

3.2. QE decay tendency and recovery status for reflective-mode photocathode

The tested sample was Mg-doped reflection-mode GaN, doping concentration was 1.37×10^{17} cm^{-3}. The Cs/O activation was performed in the UHV chamber, in which the cesium source was kept continuous and the oxygen source was introduced periodically [22]. QE curve was tested immediately after the complete activation at the original site [23]. The cathode was placed in vacuum system for 6 hours before being tested QE decay tendency. Changes of QE curves decay tendency are shown in Fig. 3. It can be seen that 6 hours later, the overall QE curve declined after complete activation. The QE decay is obvious, and the decline magnitude at short waves is small, while at long waves is a bit greater, suggesting the loss of QE at short waves is more than that at long waves.

For the QE declinement caused by the decrease of equivalent dipoles is partially reversible, and supplement with Cs can repair some destroyed dipoles, then the number of dipoles important to electrons escaping externally will increase, consequently, the descendant cathode sensitivity gets partial recovery [24]. To better understand the quantum efficiency recovery tendency and find out the effect of Cs on cathode activation, we recaesiated the cathode having been decayed, finally got the test result, and it shows the photocurrent recovers with Cs increasing. The QE curves of NEA GaN photocathode at different states is shown in Fig. 3. There was a good recovery on the overall curve, the short wavelengths below 300nm recovered better. From Table 2 it can be seen those long ones excess 300nm recovered up to 88%, which demonstrates supplement with Cs is well conductive to QE recovery.

Table 2. QE of first activation and supplement with Cs

Wavelength/nm	230	255	300	350	360	375	400
After activation QE/%	37.40	30.17	20.85	10.81	7.47	1.17	0.19
After supplement with Cs QE%	37.40	29.59	19.59	9.90	6.56	1.03	0.09

The cathode QE decayed several hours later after successful Cs/O activation, this can be attributed to the decrease of equivalent diploes important to electrons escaping externally. The QE could well recover when supplied with Cs. This suggests that when recaesiated, the destroyed diploes caused by Cs desorption are repaired, making the QE at wavelengths below 300nm partially recover. Why the QE not totally recover is that some thoroughly destroyed diploes can not recover. Meanwhile, the result suggests that the degree of recovery decreases with wavelength increasing, this is linked with surface barrier changes. As depicted in Fig. 4, surface barrier is composed of two straight lines with different slopes. The first dipole ([GaN (Mg): Cs]) marked in Fig. 2 formed during Cs-alone activation process which formed the first barrier (I), the vacuum level is lowered to NEA state. The introduction of oxygen and the Cs-only dipole layer form a Cs-O dipole layer, which is called the second barrier (II). After supplement with Cs, the band structure and surface barrier shapes change with recaesiation, the width and end height of two barriers can return to the original activation site at a degree, as shown in Fig. 4, finally making QE recovery. But because of damaged dipole caused by impurities absorption, the width and end height of two barriers can not recover totally. The barrier shape after recovery impacts more on QE of low energy electrons at long wavelength, and it is just the reason the recovery magnitude decreased with wavelength increasing.

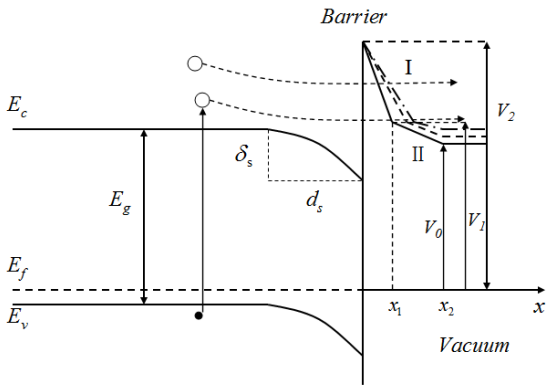

Fig. 4. Schematic surface barrier and energy band variations of R-mode NEA GaN photocathode. E_c is the conduction band minimum, E_v is the valence band maximum, E_f is the Fermi level, E_g is the band gap, δ_s is surface energy band bending, d_s is the width of Band Bending Area,V_0 and V_1 is the end height of barrier (Ⅰ) and (Ⅱ) respectively.

3.3. Band structure

The energy band structures of different surface models after scissors operator correction are shown in Fig. 5, where the dotted lines represent Fermi level. From the band structures, it can be seen that the bottom of conduction band and the valence band top of GaN are located in the G point of the Brillouin zone. The phenomenon indicates that GaN is a direct band gap semiconductor in these five conditions. After adsorption, it appears a new energy level between the conduction bands and valence bands. And the wide width of new energy level illustrates that the effective mass of electrons in it is smaller, non-locality is stronger, as a result, the electrons can move more easily at the surface. It shows that all the surface models exhibit metallic conductivity properties. From the five figures, it can be seen that Fig. (a), Fig. (c), and Fig. (e) have the similar overall shapes, while Fig. (b) and Fig. (d) have the similar shape, which indicates that Cs activation and Cs-O activation have the same effect on the photocathode, but excess Cs adsorption has the opposite effect, and appropriate Cs adsorption can improve the activation performance.

Combined Fig. 6 with the Fig. 3 and Fig. 4, the QE recovery mechanism is clear. After Cs-only activation, the formed [GaN(Mg):Cs] dipoles improve the electrons escape probability, while with the Cs atom increasing, it appears Cs desorption phenomenon. When O modules were introduced, [Cs: O] dipoles formed, which lowers the work function and promotes the photoemission, thus improving the QE. However, if the O source is continuous, excess O modules increase the work function and undermine the photocathode, which reduces the QE. After supplement with Cs, the Cs atoms combine with excess O modules, forming [Cs: O] dipoles, the QE recovered.

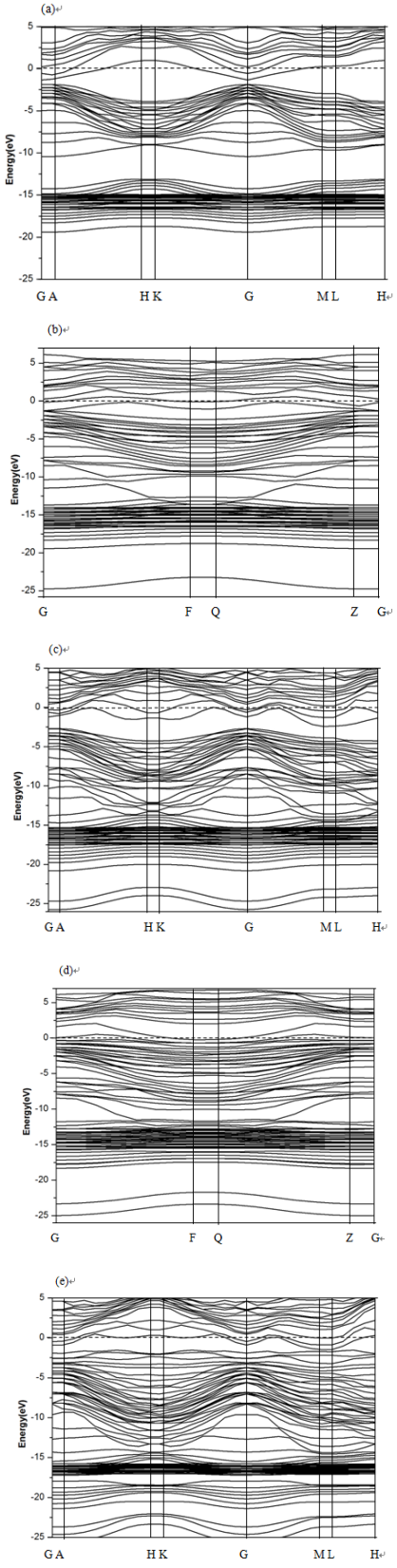

Fig. 5. Band structures of (a) clean GaN (0001) surface, (b) GaN –Cs surface, (c) GaN -Cs-Cs surface, (d) GaN-Cs-Cs-O surface, (e) GaN -Cs-Cs-O-Cs surface

4. Conclusions

In conclusion, using the first-principle density functional theory, we calculated the work function and band structures of five different adsorption models. To find out the QE recovery mechanism of NEA GaN photocathode, experiments on reflection-mode NEA GaN photocathode were performed, the QE recovery tendency was discussed. From the QE recovery curve, it can been seen there is a good recovery on the overall curve, the short wavelengths below 300nm recover better, and those long ones excess 300nm can also recover up to 88% after Cs supplement. Combined with the changes of band structure and surface barrier before and after recovery, we found out QE curve recovery mechanism. Those equivalent dipoles important to electrons escape externally are destroyed in the decay process, but can be repaired partially after supplement with Cs, and then the width and end height of barrier (I) and (II) can almost return to the original activation site. Consequently, the changes of two barriers lead to certain QE curve recovery. Combining experimental calculation with theoretical analysis can help to well study QE recovery of GaN photocathode in the future research, and then optimize its lifetime.

Acknowledgements

The authors would like to thank Meishan Wang of School of Information and Electrical Engineering, Ludong University for first principle calculations. This work was supported by the National Natural Science Foundation of China under Grant (Nos.61308089 and 61440065), Public Technology Applied Research Project of Zhejiang Province (No.2013C31068), Applied Research Project of Zhejiang Provincial Education Department (Nos.Y201432598 and 201328587) and China Postdoctoral Science Foundation funded project (No.2014M551596).

References

[1] A. S. Fremsin, O. H. W. Siegmund, Proc. SPIE **5920**, 592001 (2005).
[2] T. Maruyama, A. Brachmamn, J. E. Clendenin, T. Desikan, E. L. Garwin, E. Kirby, D-A. Luh, J. Turner, R. Prepost, Nucl. Instrum. Methods Phys. Res. A **492**, 199 (2002).
[3] O. Sirgmund, J. Vallerga, J. Malloy, A. Tremsin, A. Martin, M. Ulmer, B. Wessels, Nucl. Instrum. Methods. Phys. Res. A **569**, 89 (2006).
[4] X. Q. Fu, B. K. Chang, B. Li, X. H. Wang, J. L. Qiao, Acta. Phys. Sin. **60**, 823 (2001).
[5] F. Machauca, Z. Liu, J. K. Maldnado, S. T. Coyle, P. Pinanetta, R. F. W. Pease, J. Vac. Sci. Technol. B **22**, 3565 (2004).
[6] Z. Liu, F. Machauca, P. Pinanetta, W. E. Spicer, R. F. W. Pease, Appl. Phys. Lett. **85**, 1541(2004).
[7] O. Siegmund, J. Vallerga, J. Mcphate, J. Malloy, A. Tremsin, A. Martin, M. Ulmer, B. Wessels, Nucl. Instrum. Methods. Phys. Res. A **567**, 89 (2006).
[8] S. Uchiyama, Y. Takagi, M. Niigaki, H. Kan, Appl. Phys. Lett. **86**, 103511 (2005).
[9] Z. Liu, Y. Sun, F. Machauca, P. Pinanetta, W. E. Spicer, R. F. W. Pease, Vacuum. Sci. Technol. B (Microelectron. Nanometer Struct) **21**, 1953 (2003).
[10] X. Q. Du, Y. J. Du, B. K. Chang, Proc. SPIE **5209**, 201 (2003).
[11] L. H. Guo, J. M. Li, X. Hou, Semicond. Sci. Technol. **4**, 498 (1989).
[12] M. Milanova, A. Mintairov, V. Rumyantsev, K. Smekalin, J. Electron. Mat. **28**, 35 (1999).
[13] Y. J. Du, B. K. Chang, X. Q. Fu, B. Li, J. J. Zhang, Optik **123**, 800 (2012).
[14] J. L. Qiao, B. K. Chang, Y. S. Qian, X. Q. Du, X. H. Wang, X. Y. Guo, Acta. Phys. Sin. **60**, 017903-1 (2011).
[15] Y. J. Du, B. K. Chang, X. H. Wang, J. J. Zhang, B. Li, M. S. Wang, Appl. Surf. Sci. **258**, 7425 (2012).
[16] J. Perdew, A. Zunger, Phys. Rev. B **23**, 5048 (1981).
[17] J. Perdew, K. Burke, Ernzerh of M. Phys. Rev. Lett. **77**, 3865 (1996).
[18] M. B. Taylor, G. D. Barrera, N. L. Allan, T. H. K. Barron, Phys. Rev. B **56**, 14380 (1997).
[19] T. Lei, T. D. Moustakes, R. J. Graham, Y. He, S. J. Berkowitz, J. Appl. Phys. **71**, 4933 (1992).
[20] A. L. Rosa, J. Neugebauer, Phys. Rev. B **73**, 205346 (2006).
[21] T. U. Kampen, M. Eyckeler, W. Mönch, Appl. Surf. Sci. **123**, 28 (1998).
[22] J. L. Qiao, S. Tian, B. K. Chang, X. Q. Du, P. Gao, Acta Phys. Sin. **58**, 5847 (2009).
[23] J. L. Qiao, B. K. Chang, Y. S. Qian, X. Q. Du, Y. J. Zhang, P. Gao, X. H. Wang, X. Y. Guo, J. Niu, Y. T. Gao, Acta Phys. Sin. **59**, 3577(2004).
[24] J. J. Zou, Ph. D. Dissertation (2007 Nanjing University of Science and Technology).

*Corresponding author: 877014112@qq.com